Draft version April 12, 2025
Typeset using LaTeX **twocolumn** style in AASTeX631

The Impact of Bar Kinematics on Morphology and AGN Activity in Galaxies

Aaryan Thusoo,[1] Tobias Géron,[2] and Maria Drout[1]

[1] *David A. Dunlap Department of Astronomy & Astrophysics, University of Toronto, 50 St. George Street, Toronto, ON, M5S 3H4, Canada*

[2] *Dunlap Institute for Astronomy & Astrophysics, University of Toronto, 50 St. George Street, Toronto, ON M5S 3H4, Canada*

ABSTRACT

We present a statistical analysis of 210 galaxies identified as having prominent bar structures based on classifications from Galaxy Zoo (GZ). The kinematic properties of these bars were compared to key morphological features to identify potential correlations. Galaxies were categorized as fast-rotating if $\mathscr{R} < 1.4$ and slow-rotating otherwise, where $\mathscr{R}$ represents the ratio of the corotation radius to the bar radius. Using the Galaxy Zoo catalogue, we computed single-value metrics to quantify bulge prominence and spiral arm tightness, ranging from 0 to 1. Distributions of these values for fast and slow bars were examined to assess morphological differences. Slow bars have significantly tighter spiral arms (3.27σ, Anderson-Darling test) than fast bars. A possible trend toward smaller bulges in slow bar systems was also observed, though the difference is not statistically significant (2.89σ). Expanding the sample size could help resolve this uncertainty. We also compared AGN fractions using the MaNGA AGN catalogue. Fast bars show a higher AGN incidence ($5.71\%^{+4.13\%}_{-1.65\%}$) compared to slow bars ($3.57\%^{+2.25\%}_{-0.99\%}$), though overlapping confidence intervals limit the significance of this difference.

1. INTRODUCTION

Galaxies exhibit a range of structures and are commonly classified under the Hubble Tuning Fork scheme. A large fraction contains central bar features (Hoyle et al. 2011). One unresolved question is whether bars contribute to the quenching of star formation or are more likely to form in already quiescent galaxies. Studies have supported both interpretations (Carles et al. 2016).

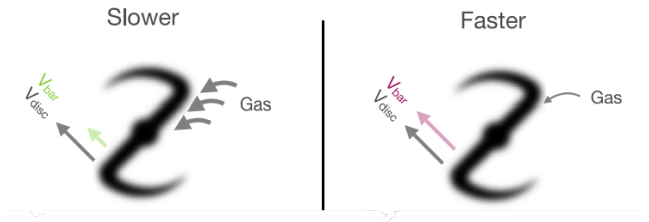

Figure 1. Simple sketch describing the efficiency of gas inflow based on the speed of the bar. This figure was obtained and modified from Géron et al. (2024)

Recent work has linked bar kinematics to central star formation rates (Géron et al. 2024). Galaxies with slower bars exhibit higher rates of central star formation. This may be due to enhanced gas inflow facilitated by the bar. This mechanism would affect star formation and influence other structural features such as bulge size, spiral arm configuration, and AGN activity. Figure 1 provides a toy model of the paper's results. Slow bars rotate slower than the surrounding disc, while fast bars rotate with velocities similar to the galaxy's disc.

We quantify relative bar speed using the dimensionless parameter $\mathscr{R}$. It is a ratio between the corotation radius R_{CR} and the bar radius. The corotation radius is where stars rotate at the same speed as the bar's pattern speed. Following Géron et al. (2023), bars are defined as slow if $\mathscr{R} > 1.4$, fast if $1.0 < \mathscr{R} < 1.4$, and ultra-fast if $\mathscr{R} < 1.0$. In this study, ultra-fast bars are included in the fast category.

2. DATA

Bar pattern speeds and corresponding $\mathscr{R}$ values for 210 galaxies were obtained from Géron et al. (2023), who applied the TW method to barred galaxies identified by Galaxy Zoo (GZ). The TW method is used to calculate the pattern speed of the bar. It uses stellar velocity and brightness data obtained through MaNGA (Bundy et al. 2015). Then, by making assumptions about the rotation curve of the host galaxy, they obtain the corotation radius. Finally, they can estimate $\mathscr{R}$ if they have measurements of the bar's radius. Géron et al. (2023) measure their bar lengths by visually inspecting the galaxy images in the DESI survey (Dey et al. 2019). Galaxy identifiers were used to cross-match with additional datasets.

2.1. *Galaxy Zoo*

Galaxy Zoo is a citizen science project that leverages volunteer classifications and machine learning to characterize the morphology of millions of galaxies (Lintott et al. 2008). This study uses classifications from GZ DESI (Walmsley et al. 2023), which contains morphological data for approximately 8.67 million galaxies. Volunteers answer a series of structured questions for each galaxy, covering bar strength, bulge size, and spiral arm structure. The survey follows a decision tree structure and returns a vote fraction for every answer. Machines are trained on the volunteer classifications to determine various morphology vote fractions for the 8.67 million galaxies. In this paper, the machine-analyzed data is used.

2.2. *MaNGA AGN Catalogue*

MaNGA provides spatially resolved spectroscopy for ∼10,000 galaxies using integral field units (IFUs). Each spaxel contains a complete optical spectrum. This enables spatially detailed measurements of galactic properties (Bundy et al. 2015). Comerford et al. (2024) identified AGN in this sample using multiple techniques. The first method uses infrared colours from the Wide Field Infrared Explorer (WISE) to identify AGN (Wright et al. 2010). The Swift Burst Alert Telescope (BAT) uses hard X-rays for detection (Oh et al. 2018). The third method is the Faint Images of the Radio Sky at Twenty Centimeters survey (FIRST), which uses radio bands observed by the NRAO Very Large Array (Becker et al. 1995). Lastly, using the Sloan Digital Sky Survey they look at broad line regions (Oh et al. 2015). Each technique is sensitive to different AGN signatures. Thus, a galaxy is classified as AGN-hosting if any of these four methods return a positive detection.

3. METHODOLOGY

The galaxies were divided into fast and slow categories based on their $\mathscr{R}$ values. Galaxy Zoo assigns bulge prominence into five bins: dominant, large, moderate, small, and none. To compute a single-value bulge metric, we adapted a formula from Garland et al. (in prep). They use a weighted formula shown in Equation 1 where B_{avg} is the single-value metric for bulge prominence. Higher values reflect more prominent bulges.

$$B_{avg} = (1.0 \times \text{dominant}) + (0.8 \times \text{large}) + (0.5 \times \text{moderate}) + (0.2 \times \text{small}) + (0.0 \times \text{none}) \quad (1)$$

Spiral tightness is assessed through a separate question in GZ. It is contingent on the initial identification of visible spiral arms. We only include galaxies with a spiral visibility score exceeding 70%. A spiral tightness value, S_{avg}, is then calculated using a similar weighted formula from Hoyle et al. (2011), shown in Equation 2.

$$S_{avg} = (1.0 \times \text{tight}) + (0.5 \times \text{moderate}) + (0.0 \times \text{loose}) \quad (2)$$

To better understand the physical representation of B_{avg} and S_{avg}, Figure 2 shows sample pictures. These show what different ranges of values correlate to for physical galaxies. This also acts as a confirmation that the formulas used are accurate representations of the bulge prominence and spiral tightness.

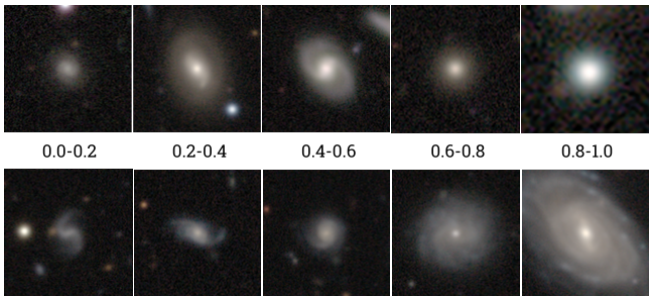

Figure 2. Sample pictures of galaxies falling into various ranges of bulge prominence (top row) and spiral tightness (bottom row) are shown. Pictures are taken at 63.6 by 63.6 arcsecs and are developed using data from the DESI survey (Dey et al. 2019)

We matched the galaxies to the MaNGA AGN catalogue to compare AGN incidence across bar types. AGN fractions were calculated for each category. Confidence intervals were derived using the beta distribution quantile method (Cameron 2011), which provides robust bounds on proportions in small or binomial samples.

4. RESULTS

4.1. *Bulge Prominence*

This section compares the bulge prominence distributions of fast and slow bars. Figure 3 shows the normalized distributions of both cases. Galaxies with slow bars exhibit a higher concentration at smaller bulge values. Their median bulge prominence is lower than galaxies with fast bars, indicating a trend toward smaller bulges.

The fast bar distribution displays a secondary peak at higher bulge values, potentially resulting from including ultra-fast bars in this group. An Anderson-Darling test returns a significance level of 2.89σ below the conventional 3σ threshold. Therefore, while suggestive, this result is not statistically significant. Increasing the sample size may reduce uncertainties.

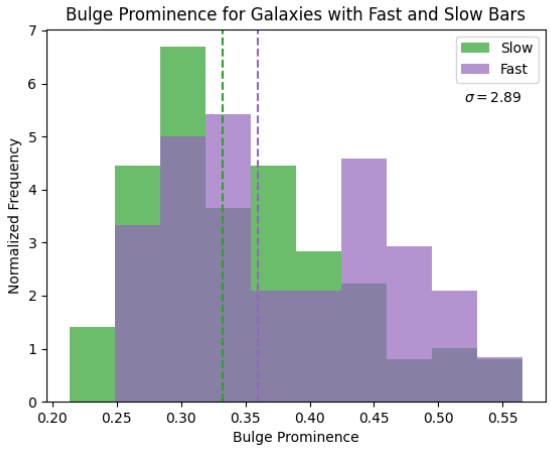

Figure 3. Distributions of bulge prominence for fast (purple) and slow (green) bar galaxies. The shape shows slow bars with smaller bulges, although statistical analysis indicates this is insignificant at only 2.89σ.

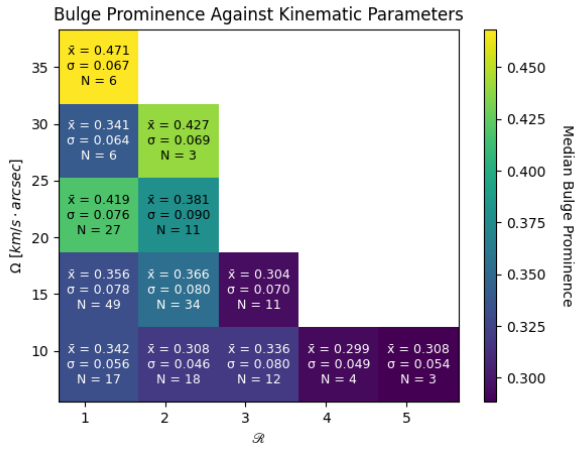

Figure 4. Two-dimensional histogram of bulge prominence across $\mathscr{R}$ and Ω. Color indicates the median value. Each bin also shows mean ($\bar{x}$), standard deviation (σ), and sample size (N).

To further assess potential kinematic influences, we incorporate the absolute bar pattern speed in our analysis. Figure 4 does this using a two-dimensional histogram. Each bin is colour-coded by the median bulge value and annotated with the mean, standard deviation, and sample count.

Higher bulge values are concentrated in the upper left corner, corresponding to bars with both high absolute and relative speeds. The lower right, representing bars with slower kinematics, contains lower median and mean bulge prominence values. A gradual decline in bulge prominence is observed when moving diagonally from the top left to the bottom right, suggesting a weak trend tied to bar kinematics.

We further divide the sample by bar strength, yielding four subgroups. Figure 5 displays their normalized bulge distributions. The shapes of the histograms are consistent within the fast and slow groups, regardless of bar strength. No pairwise comparison among these groups yields significance above 2σ, indicating that bar strength alone does not appear to influence bulge prominence.

These results do not support the gas inflow hypothesis, which predicts more prominent bulges in slow bars due to enhanced central gas accumulation. An alternative explanation is the bulge erosion scenario proposed by McClure (in prep). In these simulations, bar pattern speeds decrease over time, suggesting that bars form with high pattern speeds and gradually slow down over time. As the bar rotates, it transfers angular momentum and may strip stars from the bulge, reducing its size. Since slow bars are associated with older systems, which have had more time to erode the bulge, smaller bulges

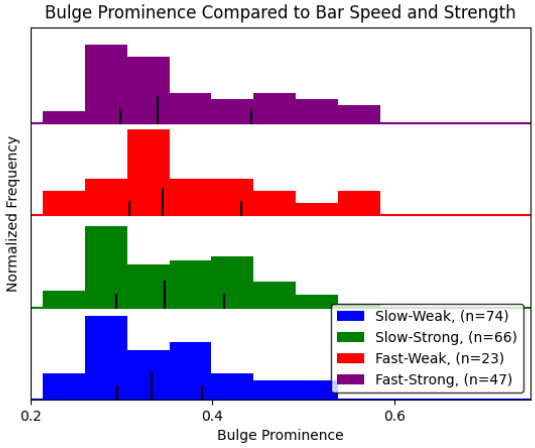

Figure 5. Normalized bulge prominence distributions split by bar speed and strength. Sample sizes are indicated. The y-axis is normalized; only the distribution shape is relevant.

are expected in galaxies with slower bars in the bulge erosion model.

4.2. *Spiral Tightness*

We apply the same fast and slow categorization to investigate spiral tightness. Figure 6 shows the resulting distributions. The Anderson-Darling test returns a value of 3.27σ, proving that slow bars are associated with tighter spiral arms.

The corresponding two-dimensional histogram (Figure 7) shows no discernible trend across bins. No correlation between relative and absolute bar velocities and spiral tightness is evident in this analysis.

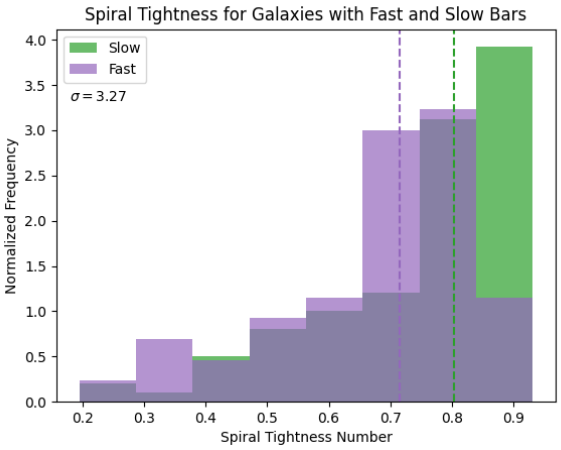

Figure 6. Distributions of spiral tightness for fast (purple) and slow (green) bar galaxies. Slow bars are associated with significantly tighter spiral arms, confirmed by the 3.27σ test.

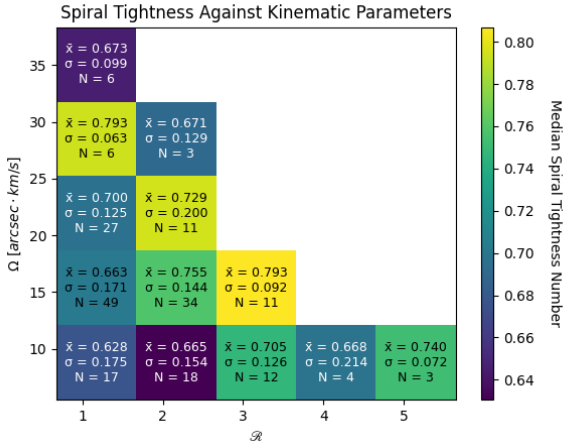

Figure 7. 2D histogram of spiral tightness across $\mathscr{R}$ and Ω. Colour represents the median value; mean ($\bar{x}$), standard deviation (σ), and sample size (N) are labelled in each bin.

To test the influence of bar strength on spiral structure, we created an additional distribution plot analogous to that used for bulge analysis. Figure 8 displays the four subgroups by speed and strength. The distribution shapes are nearly identical regardless of strength, and percentile lines overlap closely within both fast and slow categories. No pairwise comparisons return significant results, indicating that bar strength does not meaningfully impact spiral arm morphology.

Looking further at the fast categories, both contain an extended tail to looser spiral arms. This likely lowers the median of the galaxies with fast bars compared with the median of galaxies with slow bars. This result is consistent with Figure 6, where the median of galaxies

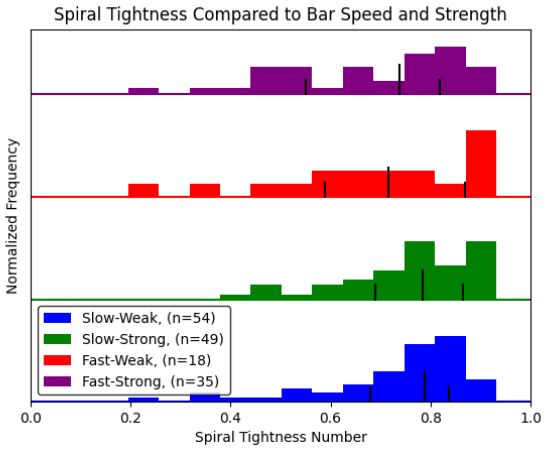

Figure 8. Normalized spiral tightness distributions for slow/fast and weak/strong bar galaxies. Sample counts are labelled. The Y-axis is normalized.

with fast bars was less than the median of galaxies with slow bars.

4.3. *AGN Rates*

Table 1 summarizes AGN for each detection method. Differences in total sample size yield different AGN incidence rates. Using the beta distribution quantile method, we estimate AGN fractions of $3.57\%^{+2.25\%}_{-0.99\%}$ for galaxies with slow bars and $5.71\%^{+4.13\%}_{-1.65\%}$ for galaxies with fast bars. These fractions are determined by using all detection methods. Based on the gas inflow hypothesis, we expected galaxies with slow bars to have a higher rate of AGN. This does not seem to be the case, as the rate is higher for fast bars. However, the overlapping uncertainty intervals suggest this difference is not statistically significant. A larger sample size will be crucial for clarifying this.

	WISE	BAT	FIRST	BROAD	TOTAL
Slow	3	2	1	3	5
Fast	3	0	0	1	4

Table 1. Number of AGN detections among slow and fast bar galaxies for each method. Total found AGN is shown, and some galaxies had confirmed detections from multiple methods.

5. CONCLUSION

Galaxies with slow bars have higher amounts of star formation, which was explained by Géron et al. (2023). They explained this by the more efficient gas inflow in galaxies with slow bars than in galaxies with fast bars. This suggests that bar-driven gas inflow may affect other

galaxy properties. Based on this hypothesis, we expected slower bars to be associated with more prominent bulges and higher AGN activity due to more efficient gas inflow. However, the results presented in this work challenge this expectation.

Another hypothesis must be developed to match better the results found in this paper. Although slow bars are linked to tighter spiral arms with high statistical confidence, they appear to host smaller bulges and lower AGN fractions. This is the opposite of what was expected in the gas inflow hypothesis. The significance of our results is also important to note. While we see the trend of slow bars hosting smaller bulges, the bulge prominence falls short of statistical significance (2.89σ). Our AGN fractions also disprove our hypothesis, but this is not a confident result as the bounds of the two fractions contain significant overlap. Increasing the sample size by applying Tremaine-Weinberg measurements on more barred galaxies would better determine whether the data has significance.

One newer explanation for the bulge prominence results is the bulge erosion hypothesis. This model aligns more closely with our observations, as slow bars are generally found in older galaxies, which would have had more time to erode the bulge. Future studies should expand the sample size and further explore the evolutionary history of bar kinematics to test this scenario more robustly.

REFERENCES

Becker, R. H., White, R. L., & Helfand, D. J. 1995, ApJ, 450, 559, doi: 10.1086/176166

Bundy, K., Bershady, M. A., Law, D. R., et al. 2015, ApJ, 798, 7, doi: 10.1088/0004-637X/798/1/7

Cameron, E. 2011, PASA, 28, 128, doi: 10.1071/AS10046

Carles, C., Martel, H., Ellison, S. L., & Kawata, D. 2016, Monthly Notices of the Royal Astronomical Society, 463, 1074–1087, doi: 10.1093/mnras/stw2056

Comerford, J. M., Nevin, R., Negus, J., et al. 2024, ApJ, 963, 53, doi: 10.3847/1538-4357/ad1a15

Dey, A., Schlegel, D. J., Lang, D., et al. 2019, AJ, 157, 168, doi: 10.3847/1538-3881/ab089d

Géron, T., Smethurst, R. J., Lintott, C., et al. 2024, ApJ, 973, 129, doi: 10.3847/1538-4357/ad66b7

—. 2023, MNRAS, 521, 1775, doi: 10.1093/mnras/stad501

Hoyle, B., Masters, K. L., Nichol, R. C., et al. 2011, Monthly Notices of the Royal Astronomical Society, 415, 3627–3640, doi: 10.1111/j.1365-2966.2011.18979.x

Lintott, C. J., Schawinski, K., Slosar, A., et al. 2008, MNRAS, 389, 1179, doi: 10.1111/j.1365-2966.2008.13689.x

Oh, K., Yi, S. K., Schawinski, K., et al. 2015, ApJS, 219, 1, doi: 10.1088/0067-0049/219/1/1

Oh, K., Koss, M., Markwardt, C. B., et al. 2018, ApJS, 235, 4, doi: 10.3847/1538-4365/aaa7fd

Walmsley, M., Géron, T., Kruk, S., et al. 2023, MNRAS, 526, 4768, doi: 10.1093/mnras/stad2919

Wright, E. L., Eisenhardt, P. R. M., Mainzer, A. K., et al. 2010, AJ, 140, 1868, doi: 10.1088/0004-6256/140/6/1868